FINITE-DIFFERENCE ANALYSIS OF SHELLS IMPACTING RIGID BARRIERS

S. D. PIROTIN, E. A. WITMER

Department of Aeronautics and Astronautics,
Massachusetts Institute of Technology, Cambridge, Massachusetts 02139, U.S.A.

SUMMARY

Nuclear power plants must be protected from the adverse effects of missile impacts. A significant category of missile impact involves deformable structures (pressure vessel components, whipping pipes) striking relatively rigid targets (concrete walls, bumpers) which act as protective devices. The response and interaction of these structures is needed to assess the adequacy of these barriers for protecting vital safety related equipment.

The present investigation represents an initial attempt to develop an efficient numerical procedure for predicting the deformations and impact force time-histories of shells which impact upon a rigid target. The general large-deflection equations of motion of the shell are expressed in finite-difference form in space and integrated in time through application of the central-difference temporal operator. The effect of material nonlinearities is treated by a mechanical-sublayer material model which handles the strain-hardening, Bauschinger, and strain-rate effects. The general adequacy of this shell treatment has been validated by comparing predictions with the results of various experiments in which structures have been subjected to well-defined transient forcing functions (typically high-explosive impulse loading). The "new" ingredient addressed in the present study involves an accounting for impact interaction and response of both the target structure and the attacking body.

The impact capability of the code consists of two basic components:

(a) an inspection technique which determines the occurrence and location of a collision between the shell and the target.

(b) an impact force application technique which determines impact pressure based on shell penetration and penetration stiffness of the shell through the equilibrium equations to influence the response of the shell.

By this procedure, the local collision analysis is combined simply in an efficient manner with the spatial and temporal finite-different solution procedure to predict the resulting transient nonlinear response of impacting shells. Although the transient response of arbitrary shells such as elbows and other piping geometries may be studied, the axisymmetric impact response of a simple sphere against a concrete barrier is discussed with respect to existing experimental evidence. The shell code predictions agree very well with the experiment and demonstrate the efficiency of the present technique.

1. Introduction

This investigation represents an initial attempt to develop a computer code for predicting the dynamic responses of pipes, or other shell-type structures, subject to impact upon relatively rigid barriers. A need for this capability exists in the nuclear power industry wherein the complexity of installing pipe whip restraints may partially be eliminated by qualifying existing floors or walls as protection from the adverse effects of pipe whip.

The study of whipping pipes impacting relatively rigid barriers is an important example for which knowledge of interaction force characteristics are required to determine the adequacy of these barriers. Although the overall and, more likely, local response of the barrier (pulverization, crushing, cratering, cracking) may influence the impact load characteristics, treating the barrier as rigid is a logical first step for analysis, and is expected to yield conservative loads for engineering applications.

It is proposed that the relative efficiency of a thin shell code analysis, when combined with an appropriate impact capability, may form a suitable engineering basis for the evaluation of pipe rigid-barrier impact interactions. More specifically, the present investigation was initiated to determine if a thin shell analysis could be applied to predict the impact force time history for a whipping pipe striking a rigid barrier. First, an existing well-documented thin-shell response code, PETROS [1], was modified to model impacts. Since no literature on the force-time history for shell impacts was available, the PETROS predictions were compared with the deformation results from an experimental study of a moderately-thick walled steel sphere impacting a concrete barrier at high velocity. This comparison indicates the general applicability of the analysis. Next, a typical large line pipe elbow configuration undergoing high velocity impact against a rigid barrier was examined. Force and displacement time histories are presented for comparison with any alternate predictive techniques.

2. Brief Historical Review

Although there have been many papers written on the subject of impact interactions between colliding bodies, there is a scarcity of information on impact force-time histories for complex deformable geometries (pipes) striking relatively rigid barriers such as walls. The modern theory of impact began with Newton who differentiated the concepts of energy and momentum, as well as developing the concept of the coefficient of restitution which plays a critical descriptive role in the momentum theory of impact. Studies based on the momentum theory and the coefficient of restitution, however, fail to provide an understanding of the impact process and the transient exchange and transformation of energy which occur when the colliding bodies are in intimate contact. For this, the dynamic equations of equilibrium must be applied for a determination of the transient stresses and accelerations produced within the impacting bodies.

Because of the inherent complexity of generating solutions to the general equations, certain simplifying assumptions are usually imposed. Two basic approaches have been developed. The simplest type of solution initially neglects dynamic effects for the determination of the local stress distribution; the stress field in the vicinity of impact is calculated assuming linear elasticity and semi-infinite boundary conditions, as developed by Hertz [2]. Alternately, this technique may be used for systems in which the duration of impact is long compared with the time required for stress waves to propagate through the body.

The second method of approximation includes the effects of inertia, giving rise to the theory of stress wave propagation. This theory must be applied when the forces or stresses vary sufficiently rapidly during the impact process. Typical problems requiring this approach include the longitudinal and transverse impact of long beams, plates, and rods. Practical solutions involving this approach are generally restricted to simple geometries with uniform properties.

Several investigators have used a combination of both approaches to solve impact problems. Sears [3] applied the Hertz contact law to study longitudinal collisions while Timoshenko [4] used this result to investigate the transverse impact of a sphere on a beam. The method used for the current analysis may be considered an extension of this approach; that is, the local region around each mesh point is assumed to experience a uniform impact pressure within the inter-mesh region.

Recent theoretical and experimental investigations have begun to address complex impact problems of practical importance. Jones [5] has recently presented a paper reviewing some of these studies. Although principally concerned with ship collisions, he does mention critical works involving impacts of vehicles, aircraft, spheres, and cylinders.

Several computational codes are now available which contain provisions for treating impacts. Hughes [8] employs a collision capability in which two nodes on separate impacting bodies are paired for impact by attaching them with special contact elements. Wu and Witmer [9] treat impacts of rigid fragments against rings using the collision-imparted velocity method which employs a coefficient of restitution to describe the local impact interaction; it models the collision process as a sequence of incremental impacts which occur in the timewise incremental solution process. However, this momentum-based technique is strictly applicable only to a description of the relative velocity after, not during, a collision when the transformation of kinetic and internal energies is complete. Developed in that analysis is an efficient impact search procedure which was expanded by the present authors and Spilker [10] to form the current impact detection capability. Recently, Morino [11] and Lanza [12] have reported a shell impact technique which, for multi-bodied impacts, assumes a common acceleration for the points in contact, under certain conditions regarding the direction of the acceleration. Special pressure and initial impact velocity distributions must be postulated. For rigid-wall impacts, kinematic rather than dynamic impact conditions are established. The shell acceleration at the impact point is determined from the condition that the shell cannot penetrate the wall. Note that the resulting impact force is unknown, but it can be determined, as the authors [12] note, by examining the equation of equilibrium.

The impact capability presented in the current paper examines, in more detail, the local inertia and material stiffness of the shell in the region of impact, and attempts to make the impact treatment more consistent with the structural approximate model.

3. Description of PETROS

The PETROS [1] computer code is a finite difference code designed to treat the large transient deformations of thin shells subjected to transient loads; this code has since been modified to accommodate simple impact problems. The equations of dynamic equilibrium appropriate for a shell, and the corresponding boundary conditions, are obtained in a consistent manner form Hamilton's Principle as applied to a 3-dimensional body. The displacement field through the shell thickness may be described in terms of the displacement of the shell reference surface (midsurface) by

$$\bar{u}(\xi^\alpha, \zeta) = \bar{u}_o(\xi^\alpha) + \zeta\left[\bar{N}(\xi^\alpha) - \bar{n}(\xi^\alpha)\right] \tag{1}$$

where

ξ^α, ζ = Lagrangian reference surface in-plane and normal coordinates, respectively

$\bar{u}$ = Displacement at any ξ^α, ζ station

$\bar{u}_o$ = Reference surface displacement (ζ=0)

$\bar{N}, \bar{n}$ = Normal vector to deformed and undeformed reference surface, respectively.

Next, the 3-dimensional equations of stress equilibrium are integrated through the shell thickness to obtain the equations of equilibrium for the stress resultants (forces and moments) along the reference surface. These are integrated by parts to form three equilibrium equations, one for each component of u^j the reference-surface displacement $\bar{u}$ in Cartesian direction $\bar{i}^j$.

$$\tilde{M}\,\ddot{u}^j = \frac{\partial \tilde{N}^{\alpha j}}{\partial \xi^\alpha} + \tilde{F}^j \tag{2}$$

where

$$u^j = \bar{u}_o \cdot \bar{i}^j \tag{3}$$

$\tilde{N}^{\alpha j}$ = Cartesian components of the generalized (shear and inplanar) forces acting along an edge defined by ξ^α = constant.

$\tilde{F}^j$ = Generalized applied force per unit area in direction $\bar{i}^j$.

$\tilde{M}$ = Generalized mass per unit area.

$\ddot{u}^j$ = Acceleration of shell reference surface in direction $\bar{i}^j$.

The shell reference surface is represented by control stations or nodes which form a mesh or network along the ξ^α reference-surface coordinates. The finite-difference technique is employed both along the reference surface spatial coordinates ξ^α and in time t to solve the dynamic equations of equilibrium.

A preliminary impact capability, which determines at each increment the impact loading that must be added to $\tilde{F}^j$, was incorporated recently in the PETROS formulation.

3.1 Applicability of Thin Shell Theory to Process Piping Geometries

Although the PETROS [1] nonlinear shell code accurately treats thin shells, its applicability to thicker shells, such as process high energy piping, must be explored. Thin shell theory incorporates two basic assumptions: (a) the Kirchhoff hypothesis which states that the normals to the shell midsurface remain straight and normal to the deformed midsurface and (b) the stress field is essentially two-dimensional (transverse shear deformation and ζ-direction normal stresses are ignored).

Although the adequacy of the Kirchhoff hypothesis for general piping geometries subject to arbitrary loads cannot be defended, unpublished test data [13] involving the uniform static indentation of short pipes between platens has demonstrated the validity of this assumption throughout the greater part of the deformation process. Only when the deformed radius of curvature approached the pipe's wall thickness or when fracture occurred did this hypothesis break down.

Defending the stress field limitation is more complex. Although only a thorough examination of the 3-dimensional equations of equilibrium within the piping could clarify this issue, one might argue that aside from its influence on the state of plasticity at the point of impact, the rapid decay of the normal stress, coupled with the insignificance of the wall thickness change, diminishes its effect in the region immediately adjacent to the contact point where the pipe develops its local crush rigidity.

For quasi-static crush, as mentioned above, the Kirchhoff hypothesis is adequate and hence transverse shear strains and stresses can also be ignored. The omission of the transverse shear stresses and strains may be of greater significance for higher velocity impacts since significant shear strains may occur in the region adjacent to the contact surface. Later analysis, employing (1) the thick-shell version of PETROS [14], which incorporates a 2-dimensional stress field, dynamic thickness changes, and transverse shear strains or (2) a complete 3-dimensional code, such as "PISCES" [6], might be necessary to verify the adequacy of the thin shell approach.

3.2 Impact Capability

The preliminary impact capability now in PETROS consists of two basic components:

(a) An inspection technique which determines the occurrence and location of a collision between the shell mesh points (nodes) and the target.

(b) An impact force application technique which determines impact pressure based on local indentation or crush of the shell surface. The user must provide a local penetration rigidity curve (pressure vs. nodal indentation). No explicit inertia term is incorporated. Inertia effects are assumed to be reflected in the force-time history.

At any time during the impact process, the target is assumed to indent locally or to penetrate the shell infinitesimally at a node; the computational procedure is carried out in small time increments Δt (with the central-difference finite-difference time operator) and all shell nodes are examined for "penetration" in the searching procedure. The penetration is employed in conjunction with the local penetration stiffness to calculate the local impact pressure at the impacting node. This impact pressure is treated as an additional loading on the shell at the midsurface. It is inserted into the incremental equations of motion, leading to a modified nodal position, velocity, and acceleration.

Based on preliminary results with the present technique and a simple spring-mass analysis of the local impact interaction, it is proposed that specification of a local penetration stiffness include the following criteria:

(1) It must be consistent with the sophistication of the theory employed to treat the colliding structures. PETROS incorporates thin shell theory. Consequently, the local penetration stiffness should reflect the local shell bending rigidity and similar phenomena associated with shell behavior.

(2) It must be consistent with the spatial approximation (mesh size $\Delta\xi^{\alpha}$) and the temporal approximation (time increment Δt). The time increment is ordinarily of the order of the critical time increment Δt_{cr} required to insure numerical

computational stability of the solution process for the shell. As the minimum mesh size $\Delta\xi$ is reduced, the (associated) critical time increment decreases since the mesh's "natural frequency" increases (the intermesh rigidity increases while the nodal mass, or inertia effect, decreases). If the penetration rigidity is to reflect the intermesh structural rigidity, it must increase with decreasing mesh and time increment size.

(3) It must reflect the condition that local inertia phenomena, on the intermesh level, are neglected in the quasi-static local penetration stiffness. To remain quasi-static, the natural period of the local spring mass system, which represents the nodal mass in combination with the penetration stiffness and the intermesh structural stiffness, should be of the order of the time increment. This condition defines a relationship between the time increment, the local penetration rigidity, and the intermesh structural rigidity. A simple analysis indicates that the local penetration rigidity should be of the order of the intermesh structural rigidity. Specifying too large a local penetration rigidity would require a time increment smaller than the time increment size which is critical to stability.

(4) It must reflect the condition of shell and barrier impenetratability; i.e., a contact surface exists (even if the bodies can locally deform, work must be done to accomplish this). Again, a simple analysis suggests that the local penetration rigidity should be of the order of the intermesh structural rigidity. Too small a local penetration rigidity, assuming that the critical time step is used, would lead to excessive penetrations. Since the problem is being solved incrementally, the incremental penetration (velocity times Δt) should be much smaller than a typical normal length, such as the shell thickness h.

The following method for determining an appropriate theory, mesh size, and local crush rigidity might be considered:

Low Velocity Impacts: The shell ovalizes upon impact and the deformation gradients are smooth. Because of this, relatively large mesh spacings (with respect to shell thickness) may be utilized with a thin-shell theory. A stiffness of the order of the inter-meshing bending rigidity would be employed as the local crush rigidity. This meets conditions 1 to 4 above.

High Velocity Impacts: The shell will experience greater displacement gradients in the vicinity of the collision. Since transverse shear strains might develop, a thick-shell code (Ref. 7) might have to be employed. Likewise, smaller mesh sizes might be required. This would not only aid in accurately predicting the displacement gradients, but also, for the present impact technique, would enable the mesh to have the high natural frequency needed to fulfill the impenetrability requirement (condition 4) in a local quasi-static manner (condition 2). The intermesh rigidity (condition 3) corresponding to the appropriate shell theory (condition 1) would determine the local crush rigidity.

Very High Velocities: Here the fine meshes required for a quasi-static treatment of local impact may lead to an inter-mesh structural rigidity which exceeds the crush rigidity of the shell wall (assuming uniform crush in the vicinity of the node). Since PETROS can allow for infinitesimal, quasi-static wall-thickness changes, the inter-mesh wall crush rigidity should be employed as the local crush rigidity. Note that this feature extends PETROS beyond the normal range of thin shell theory applicability. Alternately, the thick shell theory of Ref. 7, which allows for a first-order approximation to the thickness-change dynamics, may find application here.

Extremely High Velocities: Dynamic effects through the shell wall can no longer be ignored or approximated simply. A 3-dimensional analysis incorporating a 3-dimensional mesh must be employed. The inter-mesh rigidity would be used to determine the local crush rigidity for meshes along the impact contact boundary. Again, to insure quasi-static local crush and impenetratability at extremely high velocities, certain restraints would be placed on the size of the spatial mesh.

If one is restricted by cost considerations, for example, to employing large-size meshes for high-velocity impact problems, a momentum-based technique might be considered since the lumped inertia effects at each node dominate the behavior. Alternately, an artifically high crush rigidity may be employed with the current technique to insure that the impenetratability condition is not violated by the high velocity nodes. In either case, accuracy and convergence is questionable. Alternate approaches might have the code select impact crush rigidities based upon the particular impact velocity, mesh size, and the instantaneous state of plasticity associated with each impacting node.

The present impact technique may be applied directly to study multi-body impacts. When two bodies collide, the relative penetration into each and the local impact pressure can be determined from their respective crush curves. Friction can also be included. Each of the bodies is then subject to equal but opposite loads. Although the contact boundary (defined where the two outer surfaces coalesce) has a common position, velocity, and acceleration (while they remain in contact), the reference surfaces or centers of mass of the two colliding bodies need not share these same kinematic quantities for the high velocity case where the shell thickness is allowed to change infinitesimally.

Since some of the above arguments question the applicability of shell codes for treating "higher velocity" impacts, the present preliminary investigation was initiated to determine the feasibility of employing PETROS for predicting the transient impact forces generated by a whipping pipe as it strikes a rigid barrier at velocities of practical interest.

4. Sphere Impact

Preliminary comparisons were made between PETROS predictions and NASA test data [14] for spheres impacting against rigid barriers at velocities of ≈4700 in/sec.

Only high speed photographs of the sphere impact deformation and the final deformation shapes were reported, with no measured force-time histories during impact. Comparison of these experimental deformations with a 20 mesh axisymmetric simulation of the sphere impact using PETROS demonstrated excellent agreement. The following geometric and material parameters were employed: shell wall thickness $h=.625$ in; midsurface radius $R=12.3$ in; density $\rho=.738 \times 10^{-3}$ lb-sec^2/in^4; Poisson ratio $\nu=.3$; and $E=28.33 \times 10^6$ psi. The uniaxial stress-strain curve was approximated in a piecewise linear fashion with the following stress-strain (σ,ε) pairs: $\sigma_1=34{,}000$ psi, $\varepsilon_1=.0012$ in/in; $\sigma_2=70{,}000$ psi, $\varepsilon_2=.145$ in/in; $\sigma_3=90{,}000$ psi, $\varepsilon_3=.5$ in/in by the mechanical sublayer material model. The strain-rate parameters in the relation $\sigma_y=\sigma_{y_{static}}(1+|C\dot{\varepsilon}|^n)$ were $C=.0238$ sec and $n=.112$ [15]. A time increment of

$\Delta t=.33 \times 10^{-5}$ sec was employed. The minimum mesh size was 1.3 inch.

The transient deformation predictions are illustrated in Fig. 1. The final deformation (Fig. 2) of the sphere simulation agreed well with the experimental specimen after impact, indicating the "adequacy" of the thin shell treatment for this moderately-thick shell geometry.

5. Pipe Elbow Impact

As a further examination of this preliminary impact capability of PETROS, results are shown for an impacting pressurized shell consisting of a 1.5D 90° 24" SCH 80 elbow with straight lengths of pipe attached to each end of the elbow (Fig. 3a). This piping configuration was assumed to strike a rigid wall at a normal velocity of 3500 in/sec. Quarter symmetry using a 17 x 18 mesh was employed in modeling the piped-elbow for this impact geometry (Fig. 4).

The following geometric and material parameters employed were: shell wall thickness $h=1.218$ in; density $\rho=.738 \times 10^{-3}$ lb-sec^2/in^4; $\nu=.3$; and $E=26 \times 10^6$ psi. The stress-strain coordinates (σ,ε) used to model the uniaxial stress-strain curve were: $\sigma_1=26{,}000$ psi, $\varepsilon_1=.001$ in/in; $\sigma_2=42{,}500$ psi, $\varepsilon_2=.025$ in/in; $\sigma_3=65{,}000$ psi, $\varepsilon=.15$ in/in in the mechanical-sublayer material model. The strain-rate parameters employed were $C=.316$ sec and $n=.3$ [16], since high temperature conditions are present. An internal pressure of 1000 psi was applied to the interior of the shell and was held constant for the duration of the run. The pressure remained normal to the inner pipe surface as it deformed during impact. A time increment of $\Delta t=4$ microseconds was chosen.

The straight pipe lengths attached to the elbow represent a rough estimate of the additional effective piping length and mass, which must be stopped via local crush energy absorption as the elbow strikes the wall. This model is intended to demonstrate the classic unrestrained pipe whip accident as shown in Fig. 3b. The symmetric model requires less computational time and is easier to model experimentally.

Typical impact deformations of the piped-elbow, as modeled by PETROS, is shown in Fig. 4. The corresponding impact force-time history, in a very preliminary analysis, are shown in Fig. 3c. The oscillations in the force-time histories are partially mesh size dependent, but the overall curve shape and magnitude are believed to be reasonable.

6. Conclusions

Generally, good agreement was achieved between the PETROS predictions and experiment for the impact displacement-time histories and permanent deformations for the moderately-thick sphere impacting a wall at 4700 in/sec. For intensive local loadings, tranverse shear and 3-dimensional effects are expected to be significant; however, if the overall deformation pattern can very nearly be approximated by the Kirchhoff hypothesis, the thin-shell theory and its two-dimensional state of stress may be adequate for engineering purposes. This appears to be the condition for moderately-thick piping geometries striking barriers throughout the probable range of impact velocities. Should the transverse shear and other effects prove to be significant for higher velocity impacts, the thick-shell version of PETROS [7] might be employed.

The deformation and impact force-time histories from the preliminary thin-shell PETROS analysis of a piped elbow deforming against a rigid barrier appear to be plausible and can be used for comparison with other predictive techniques. Experiments designed to measure local impact force-time histories should be conducted and subsequent theoretical-experimental correlation studies carried out to provide a direct evaluation of the accuracy and adequacy of the proposed procedure.

References

[1] PIROTIN, D., BERG, B.A. and WITMER, E.A., "PETROS 3.5: New Developments and Program Manual for the Finite-Difference Calculation of Large Elastic-Plastic Transient Deformations of Multilayer Variable-Thickness Shells", BRL-CR-211, MIT, Cambridge, Mass., (also MIT ASRL TR 152-4) February 1975.

[2] HERTZ, H., "Überdie Berührung Fester Elastischer Körper", 1881, "Überdie Berührung Fester Elastischer Körper and Überdie Härte", 1882.

[3] SEARS, J.E., "On the Longitudinal Impact of Metal Rods with Rounded Ends", Trans. Camb. Phil. Soc., 21, 1908, 49.

[4] Timoshenko, S.P., Vibration Problems in Engineering, D. Van Nostrand Company, Inc., New York, 1937.

[5] JONES, N., "On the Collision Protection of Ships", International Seminar on Extreme Load Conditions and Limit Analysis Procedures for Structural Reactor Safeguards and and Containment Structures", Berlin, 1975.

[6] Anon., "PISCES Computer Code", Physics International Company, 2700 Merced St., San Leandro, Calif.

[7] PIROTIN, D., BERG, B.A. and WITMER, E.A., "PETROS 4: New Developments and Program Manual for the Finite-Difference Calculation of Large Elastic-Plastic and/or Visco-elastic Transient Deformations of Multilayer Variable Thickness (1) Thin Hard-Bonded, (2) Moderately-Thick Hard Bonded or (3) Thin Soft-Bonded Shells", BRL CR-316, MIT, Cambridge, Mass., September 1976.

[8] HUGHES, T., TAYLOR, R.L. and SACKMAN, J.L., "Finite Element Formulation and Solution of Contact-Impact Problems in Continuum Mechanics", PB-233 888, California Univeristy, Berkeley, CA., May 1974 (Report No. UCSESM 74-8).

[9] WU, R. and WITMER, E.A., "Finite-Element Analysis of Large Transient Elastic-Plastic Deformations of Simple Structures, with Application to the Engine Rotor Fragment Containment/Deflection Problem", ASRL TR 154-4, ASRL, MIT, January 1972. (Available as NASA CR 120886.)

[10] SPILKER, R., Private communication.

[11] MORINO, L. and DIENES, J.K., "PETROS 3 FITS: Formulation and Computer Program for the Analysis of Impact of Fragments on Thin Shells", Systems, Science and Software Report SSS-R-1991, December 1973.

[12] LANZA, T.T., "Normal Impact of a Shell with a Fragment and with a Rigid Wall", M.S. Thesis, Boston University, 1976.

[13] Unpublished experimental data on static crush characteristics of steel rings performed at the MIT Aeroelastic and Structures Research Laboratory.

[14] PUTHOFF, R.L. and DALLAS, T., "Preliminary Results of 400 ft/sec Impact Tests of Two 2-Foot Diameter Containment Models for Mobile Nuclear Reactors", NASA TM X-52915, Lewis Research Center, Cleveland, Ohio, October 1970.

[15] STEICHEN, J.M., "High Strain Rate Tensile Properties of AISI Type 304 Stainless Steel", Trans. ASME Journal of Engineering Materials and Technology", July 1973.

[16] KENDALL, D.P., "Effect of Strain Rate and Temperature Yielding in Steels", Journal of Basic Engineering, March 1972.

Acknowledgments

The authors wish to acknowledge the generous help and constructive advice of their colleagues John M. Peech and Robert E. Roemer.

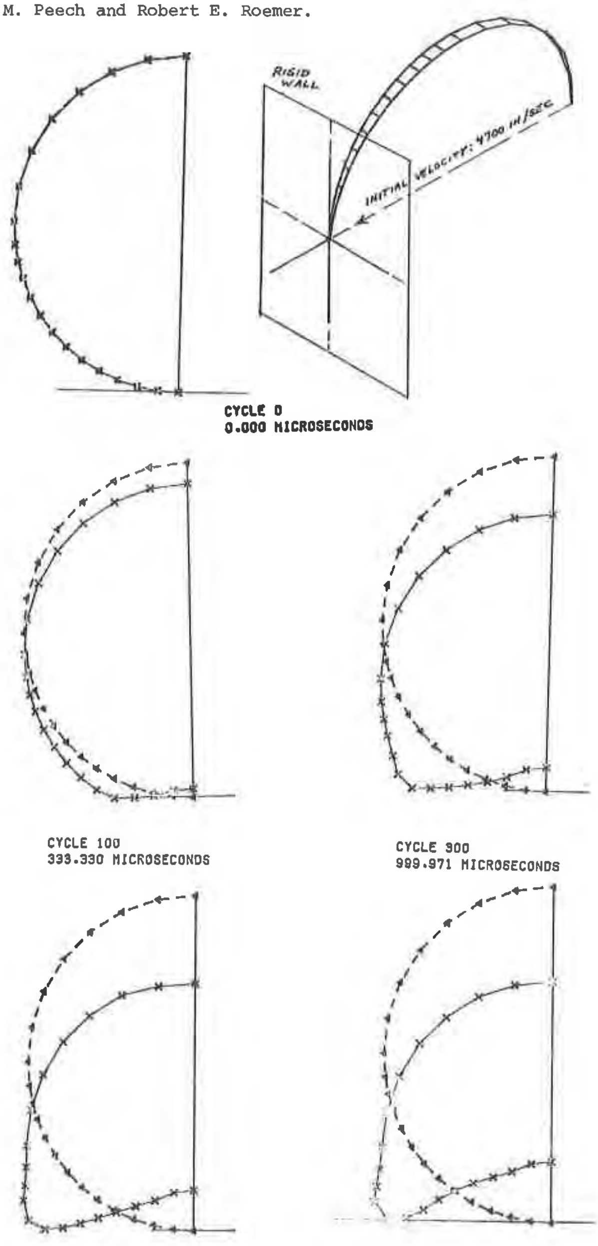

CYCLE 0
0.000 MICROSECONDS

CYCLE 100
333.330 MICROSECONDS

CYCLE 300
999.971 MICROSECONDS

CYCLE 500
1666.609 MICROSECONDS

CYCLE 1100
3666.529 MICROSECONDS

Fig. 1 Transient Deformation of a Spherical Shell Impacting a Rigid Flat Wall at 4700 In/Sec

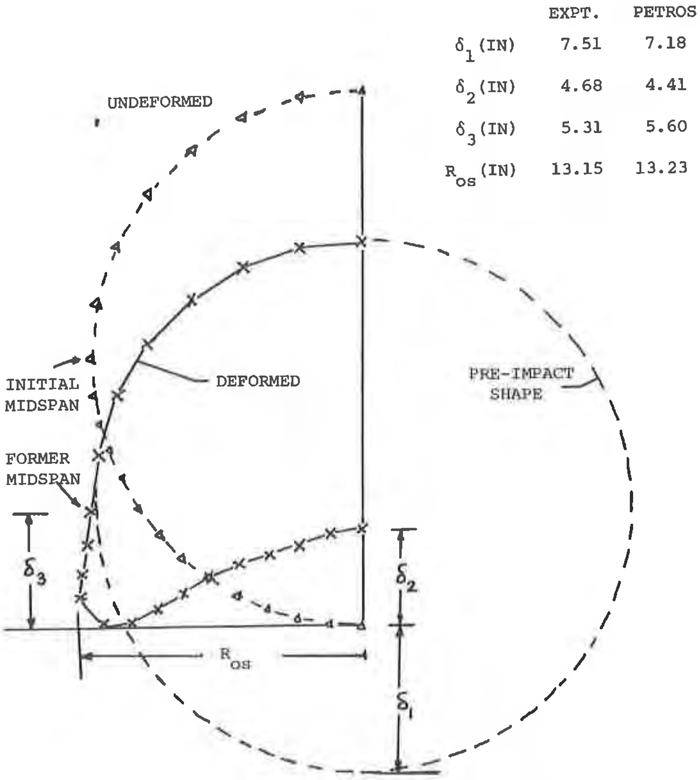

	EXPT.	PETROS
δ_1 (IN)	7.51	7.18
δ_2 (IN)	4.68	4.41
δ_3 (IN)	5.31	5.60
R_{os} (IN)	13.15	13.23

Fig. 2 Permanent Deformation of the Spherical Shell

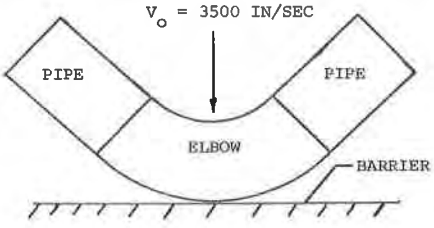

(a) PIPED-ELBOW CONFIGURATION

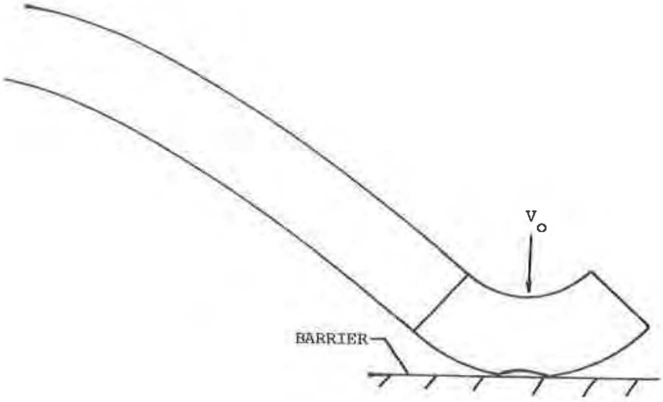

(b) IMPACT OF WHIPPING PIPE

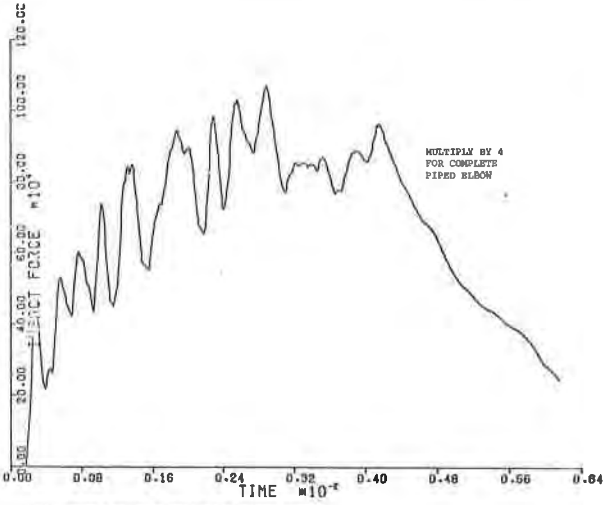

(c) IMPACT FORCE-TIME HISTORY FOR QUARTER SECTION

Fig. 3 Piped Elbow and Pipe Whip Configurations and Impact Force-Time History Applied to the Flat Rigid Wall

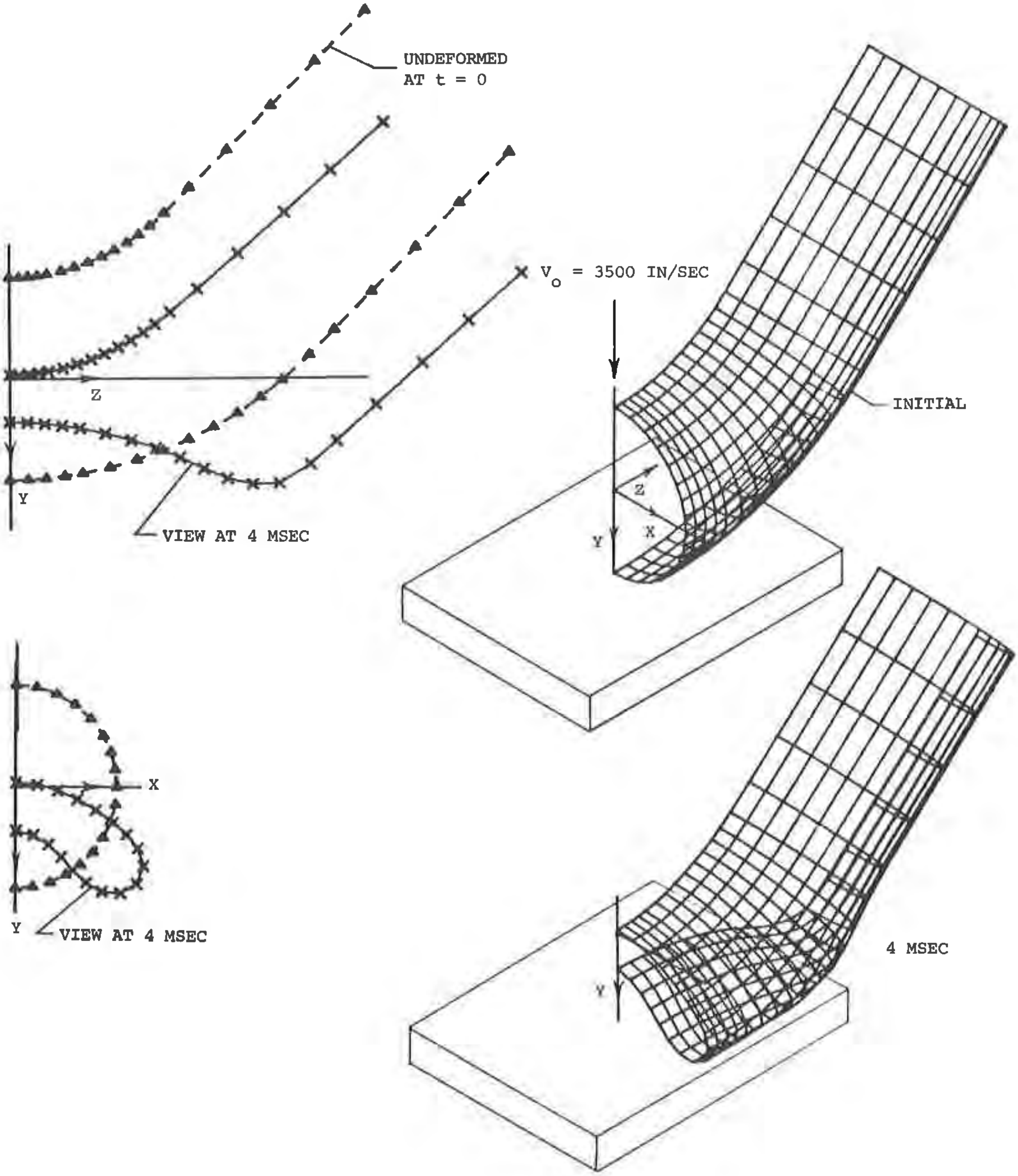

Fig. 4 Deformation of Pipe-Elbow Quarter-Section Configuration at 4 MSEC After Impact